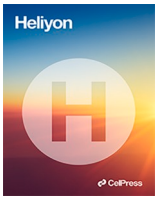
Heliyon 10 (2024) e26171



Contents lists available at ScienceDirect

Heliyon

journal homepage: www.cell.com/heliyon



Research article

An efficient ECG signals denoising technique based on the combination of particle swarm optimisation and wavelet transform

Abdallah Azzouz [a,*], Billel Bengherbia [a], Patrice Wira [b], Nail Alaoui [c], Abdelkerim Souahlia [d], Mohamed Maazouz [a], Hamza Hentabeli [a]

[a] Research Laboratory in Advanced Electronics Systems (LSEA), University of Medea, Pole Urbain, Medea, 26000, Algeria
[b] Institute of Research in Computer Science, Mathematics, Automation and Signal IRIMAS, Université de Haute Alsace, Mulhouse, 68093, France
[c] Laboratoire de Modélisation, Simulation et Optimisation des Systèmes Complexes Réels, University Ziane Achour of Djelfa, Djelfa, 17000, Algeria
[d] Telecommunications and Smart Systems Laboratory, University Ziane Achour of Djelfa, Djelfa, 17000, Algeria

ARTICLE INFO

Keywords:
Electrocardiogram
Particle swarm optimisation
Wavelet transform
AWGN
Power line interference

ABSTRACT

During the recording time, electrocardiogram (ECG) signals are subject to multiple artefact noises, such as muscle activity, white Gaussian noise (WGN), baseline wander, and power line interference (PLI). Therefore, pre-processing of ECG signals is essential to eliminate these artefacts and to obtain efficient ECG features. Many approaches have been proposed for removing ECG noises, including ECG signal denoising using wavelet transform (WT). However, the effectiveness and performance of the WT technique are strongly related to the configuration of its control parameters, which are typically fine-tuned through a laborious and time-consuming series of experiments. This paper introduces a technique that combines particle swarm optimisation (PSO) with WT for ECG signal denoising. The key contribution of this research is the use of PSO to determine the optimum settings for all WT parameters for ECG signal denoising (type of wavelet basis function Φ, thresholding function β, level of decomposition L, rule for threshold selection λ, and rescaling method ρ). The efficiency of the proposed method is evaluated using the percentage root mean square difference (PRD) and the signal-to-noise ratio (SNR), employing various ECG signals available online from the MIT-BIH Arrhythmia database. Experimental results show that the proposed PSO-WT technique yields better results than state-of-the-art techniques in terms of SNR, particularly for PLI measured at 60 Hz and still acceptable at 50 Hz. For example, a denoised ECG signal resulting from the proposed technique at an SNR input of 10 dB corresponds to an SNR_{output} of 27.47 dB at 60 Hz, improving the quality of the denoised ECG signal and making it more appropriate for clinical diagnosis. Furthermore, the proposed method also shows promising efficiency in the presence of WGN, making it highly relevant for IoT applications and RF transmission.

1. Introduction

An electrocardiogram (ECG) is a standard tool for detecting cardiovascular disorders. The ECG reflects the electrical activity of the

* Corresponding author.
E-mail addresses: azzouz.abdallah@univ-medea.dz, abdallahinttic@gmail.com (A. Azzouz).

https://doi.org/10.1016/j.heliyon.2024.e26171
Received 6 April 2023; Received in revised form 25 November 2023; Accepted 8 February 2024
Available online 14 February 2024
2405-8440/© 2024 The Authors. Published by Elsevier Ltd. This is an open access article under the CC BY-NC-ND license (http://creativecommons.org/licenses/by-nc-nd/4.0/).

cardiovascular system and is easily recorded using surface electrodes placed on the limbs or chest. The ECG signal consists of the P wave, QRS complex, and T wave, which together depict a heartbeat. The P wave represents atrial depolarisation, the QRS complex represents ventricular depolarisation, and the T wave represents ventricular repolarisation. Based on the characteristics of these waves, a subject's anomalies can also be identified. A typical ECG signal has amplitude and frequency ranges of 10 μV–5 mV and 0.05–100 Hz, respectively [1]. By recording precise information from each ECG component, the heart's physical state may be evaluated [2–4]. Unfortunately, various noises, including AC interference, faulty electrode connections, machine malfunctions, and the patient's movement and breathing, can superimpose ECG measurements [5]. These disturbances are collectively referred to as artefacts. In practice, recovering a clean ECG signal from noisy measurements is essential, and artefacts must be removed to make an accurate diagnosis. As a result, ECG signal denoising is one of the greatest challenges in biological signal processing.

The most prevalent types of noise affecting ECG are power line interference (PLI) and additive WGN (AWGN). These interfere with the ECG signal's quality and eliminate essential characteristics valuable for diagnosing heart problems. Therefore, separating the true ECG signal from artefacts is vital for visual interpretation. Despite adequate shielding, grounding, and amplification design, PLI often disrupts biomedical signals. This is because it is a high-frequency (50 or 60 Hz) noise with a randomised phase but a consistent frequency, typically caused by electrical interference from the power grid [6]. The ECG signal is often described as having an additive sinusoidal component (50 or 60 Hz) with a variable phase and a constant frequency [1]. The PLI resides within the ECG signal frequency band (0.05–100 Hz) and can alter the structure of the ECG signals. In contrast, AWGN is a basic noise model used in information theory to mimic the effect of several random processes that occur in nature.

There is a vast number of approaches described in the literature for removing ECG artefacts. Various types of digital filters, such as FIR and IIR filters, have been utilised to remove PLI from an ECG [7,8]. Each of these is based on filtering approaches that assume the ECG signals are linear and steady. Due to the non-stationary nature of ECG signals, removing interference from 50- or 60-Hz power lines using filters with fixed coefficients is challenging. The remainder of the spectrum is only minimally affected when rejecting frequencies between 50 and 60 Hz by using notch filters of a specific narrow frequency range. These techniques are inexpensive and simple to use. As a result of signal and disturbance superimposing, however, they generate undesired signal distortion. All interferences are removed; however, the essential and important frequency elements of the ECG signal are also eliminated [9].

Non-stationary signals are processed with algorithms based on the wavelet transform (WT) [10]. The WT is not adaptive; an ECG-dependent wavelet basis function is required. Various adaptive filters [11–13] and adaptive filters with notch filters [9] have been used to eliminate PLI from the ECG signal. The main drawbacks of adaptive filter-based techniques are the requirement of a reference signal and convergence to an optimal solution.

Diverse soft computing solutions, including genetic algorithms (GA) [14] and neural networks [15]-based approaches, have been presented for the elimination of PLI from the ECG signal. The computational complexity of real-time ECG analysis makes soft computing techniques unsuitable. Huang et al. [16] presented empirical mode decomposition (EMD) as a technique for processing both non-stationary and stationary signals. EMD-based signal analysis is adaptive as it extracts fundamental functions directly from the signal. Through sifting, EMD decomposes a signal into a set of amplitude modulation-frequency modulation (AM-FM) components known as intrinsic mode functions (IMFs). In EMD, the frequency content of an IMF decreases as its order increases. Various EMD-based PLI removal techniques have been studied, where the contaminated signal is divided into different IMFs and noisy IMFs are removed during ECG rebuilding. In Ref. [17], the initial IMF for EMD is employed to remove PLI noise. The filtered signal demonstrates R-attenuation as an R-wave is also found in the primary IMF alongside PLI noise. Various adaptive filters [18–20] and EMD combined with wavelet analysis [21,22] have been employed to clear up noisy IMFs and preserve ECG components.

The most significant disadvantage of EMD-based noise elimination is the mode-mixing problem. This occurs when a signal with similar scales appears in more than one IMF component or when a signal with very different scales appears in a single IMF component. As a way to solve the mode-mixing problem in EMD, a new method of analysing interference data, called ensemble EMD (EEMD), is suggested. The removal of noise from ECG signals using EEMD is discussed in Ref. [23]. Utilising the modified recurrent least squares algorithm (MRLS) [24], adaptive notch filters, and discrete-time oscillators helps reduce PLI noise in biomedical signals. Employing the least-mean-squares algorithm (LMS), the EMD-based filtering method [19] reduces the frequency of PLI. The two-weight adaptive filter uses the first IMF as a reference signal in this method. PLI noise is suppressed using the time-variable notch filter technique [25], in which a single notch filter with a time-varying quality factor and a zero initiation condition has been examined. The Hilbert Huang transformation (HHT) approach, based on adaptive EMD, is used to reduce PLI noise. HHT is employed to determine the instantaneous PLI fundamental frequency, which is then utilised to provide the internal PLI signal for the adaptive filter. Furthermore, EMD-EWT-based methods [26] to eliminate PLI noise, as well as fractal and EMD-based techniques [27] and the eigenvalue decomposition technique (EVD) [28], have been examined.

In recent years, many academics have presented methods in this field to remove AWGN from ECG signals. Kumar et al. [29] evaluated the effectiveness of the EMD approach combined with the non-local mean (NLM) method by estimating the ECG using the differential standard deviation. For performance evaluation, they employed recordings from the MIT-BIH arrhythmia database and added white and coloured Gaussian noise to the tested signals.

Based on the orthogonal matching pursuit technique and the Chebyshev window, power-efficient linear-phase non-equiripple notch filters are proposed. The FIR notch filter is computed using an orthogonal matching pursuit algorithm, and its efficiency is further increased by tuning it with a Chebyshev window. In Ref. [30], conventional filtering (CF) was proposed for signal denoising, and in Ref. [31], non-local means (NLM) have been explored. It takes into account the total signal value when calculating the denoised value of a point. Hence, NLM can fully utilise the signal's long-range correlation to complete the vibration signal-denoising operation. Unlike WT and EMD, NLM can be applied directly to uncompressed signals without the need for decomposition, which is quite convenient. However, the aforementioned methods require specialised knowledge, and the selection of hyperparameters could

dramatically impact denoising performance.

A noisy ECG is dissected into 11 IMFs in Ref. [32], as noise mostly consists of components at high frequencies. Soft thresholding is employed to preserve the extremes of the time intervals between consecutive zero crossings. Consequently, noise is reduced from the first IMFs, and the signal content is primarily retained at higher IMF levels, where the residual signal is the clean ECG. EMD decomposes the signals into several functions known as IMFs and then partially reconstructs the signals after removing noisy IMFs [33]. The drawback of this method is its significant computing cost and the time-consuming iterative implementation of IMFs.

Rakshit et al. [34] suggested an additional efficient hybrid approach for ECG denoising that combines EMD and the adaptive switching mean filter (ASMF). By employing low distortion, the benefits of both the EMD and ASMF approaches were harnessed to reduce disturbances in ECG signals. Unlike conventional EMD-based techniques, which often reject the initial IMFs or use a window-based approach to reduce high-frequency noises, a wavelet-based soft thresholding scheme was adopted. This not only reduced high-frequency noises but also preserved the QRS complexes.

Signal denoising using clustering and soft thresholding (SDCST) [35] merges wavelet thresholding and hidden Markov model (HMM) techniques. It employs an HMM to separate wavelet coefficients into two groups: the actual signal and the background noise. Then, thresholds are estimated separately for each of these groups. Han et al. [36] developed an enhanced wavelet denoising methodology dubbed 'sigmoid function-based thresholding', which represents a compromise between hard and soft thresholding. This revised wavelet thresholding method maintains the amplitudes of the primary distinctive peaks quite well.

Furthermore, a variety of optimisation techniques, such as the total variation regularised least squares problem or the associated fused lasso problem (1DTVD) [37], the genetic algorithm minimisation of a new noise variation estimate (GAMNVE) [38], and others, assist in denoising the ECG. Principal component analysis and independent component analysis are two common statistical methods described in the literature.

Recently, WT has been effectively used to denoise non-stationary signals, such as ECG and EEG [39,40]. WT typically comprises five parameters, each of a different type. The efficacy of ECG signal denoising hinges on selecting the optimal WT parameter combination. This selection is formulated as an optimisation problem with the signal-to-noise ratio (SNR) serving as the fitness function [39]. Various methods have been employed. For instance, El-Dahshan [39] combined GA and WT to create a hybrid system for denoising ECG data distorted by non-stationary disturbances. Unfortunately, the comparisons were based on a single, insufficient SNR_{input} value. Moreover, the performance of this technique should be assessed for high SNR values. Using wavelets and GAs, Saleh et al. [41] offered a novel approach to denoise biological signals, such as ECG signals. Yan et al. [42] utilised GA and sample entropy to denoise various types of noisy signals using the WT approach. However, these methods have the drawback of optimising only one or two WT parameters, which usually proves insufficient for achieving high ECG denoising performance.

Filter-based WT methods are versatile tools in signal processing and data analysis. They offer the ability to perform multiresolution analysis, extract crucial features, and reveal hidden patterns within complex datasets [43]. However, these advantages come with challenges that warrant careful consideration. One significant challenge is computational complexity, particularly as datasets grow in dimensionality or size. This could potentially lead to extended processing times and increased resource demands, impacting real-time or resource-constrained applications. Additionally, choosing an appropriate wavelet function is crucial, as it can substantially influence the results, affecting the accuracy and relevance of the extracted features. Researchers and practitioners must diligently evaluate the most suitable wavelet for their datasets and analytical objectives [39]. Ultimately, the decision to employ filter-based WT methods should be informed by a comprehensive understanding of their advantages and limitations, requiring a meticulous assessment of data characteristics and application requirements. When used judiciously, these methods can unveil valuable insights and significantly enhance data analysis and signal processing.

In this paper, we propose utilising particle swarm optimisation (PSO), which has gained widespread usage and achieved notable success in various engineering fields [44–46], to optimise discrete wavelet transform (DWT) parameters for efficient ECG signal denoising in both PLI and AWGN scenarios. Additionally, we have optimised all five DWT filter parameters: namely, the wavelet filter, the decomposed level, the scaling factor, the threshold method, and the rescaling technique. The DWT is subjected to a series of iterations to achieve the best possible ECG signal filtration performance. The results obtained are assessed using an objective evaluation based on the SNR and the percentage root-mean-square difference (PRD) metrics. As a result, and after conducting a series of experiments on the well-known MIT-BIH database, we found that the results achieved using our proposed method outperformed most of the state-of-the-art techniques in the literature.

The remainder of the paper is structured as follows: Section 2 explains the WT and denoising procedure and discusses the PSO algorithm. Section 3 discusses the proposed method for denoising ECG signals, and Section 4 presents and discusses the results obtained. Finally, the conclusions and possible future perspectives of the present work are drawn in Section 5.

2. Materials and methods

2.1. ECG noise reduction by WT

WT is a frequently used and effective technique for representing signals in both time and frequency domains. It has been effectively applied in various applications, including function selection and signal compression [47–49]. Typically, WT can be divided into two categories: DWT and continuous WT (CWT) [50]. Recently, WT has found widespread application in the processing of non-stationary signals, such as EEG and ECG, as various ECG artefact effects have been shown to be detrimental to the actual ECG signal. These artefacts are caused by muscular action and PLI [34]. This study develops a denoising wavelet approach based on WGN and PLI removal. Donoho's approach is utilised in Ref. [51] as one of the methods for DWT. Fig. 1 depicts the wavelet denoising process with

three decomposition levels ($L = 3$). Multiple coefficients are used to adjust both the high and low frequencies of the input signal to degrade the already noisy input signal, as shown in Fig. 2.

DWT is also defined as follows [52]:

$$C(a,b) = \sum_{n \in Z} x(n)\, g_{j,k}(n) \tag{1}$$

In Equation (1), $C(a,b)$ represents the dynamic wavelet coefficients, $a = 2^{-j}$, $b = k2^{-j}$, $j \in Z$, $k \in Z$, Z is the set of integers, a is the size of the time scale, b is the translation, $x(n)$ is the input ECG signal, and $g_{j,k}(n) = 2^{j/2} g(2^j n - k)$ is the DWT.

In general, there are three steps to the wavelet denoising process, which are outlined below:

- **ECG signal decomposition:** This involves splitting the original ECG signal into three levels and decomposing each level into two components – the approximation coefficients (cA) and the detail coefficients (cD), given by Equations (2) and (3), respectively. The cD is treated with a high-pass filter, while the cA continues to be deconstructed for the next level in the manner described below:

$$cA_i(t) = \sum_{k=-\infty}^{\infty} cA_{i-1}(K)\phi_i(t-K) \tag{2}$$

$$cD_i(t) = \sum_{k=-\infty}^{\infty} cD_{i-1}(K)\Psi_i(t-K) \tag{3}$$

Where $cA_i(t)$, $cD_i(t)$ represent the approximation coefficients and the detail coefficients for level i,respectively. Ψ is the scaling, and ϕ is the shifting.

- **Thresholding:** The Minimax thresholding technique in DWT is used to find the threshold values that minimise the maximum mean square error (MSE) between the original and denoised signal. These threshold values are calculated to minimise the worst-case error across all wavelet coefficients. Here is how to compute the thresholds using the Minimax criteria in DWT:

Estimate Noise Level: An estimate of the noise level present in the signal is required. This estimate can be obtained through various methods, such as calculating the standard deviation of the wavelet coefficients in the noisy signal or using statistical estimators, such as the median absolute deviation (MAD) of the coefficients. The accuracy of noise estimation is crucial for the effectiveness of Minimax thresholding.

Calculate the thresholds: For each wavelet coefficient at a specific scale and level, calculate the threshold value based on the Minimax criterion, as shown in Equation (4). The threshold (δ) for each coefficient is determined as follows [51]:

$$\delta = \begin{cases} \sigma(0.3936 + 0.1829\, log_2\,(N)), & N > 32 \\ 0, & N \leq 32 \end{cases} \tag{4}$$

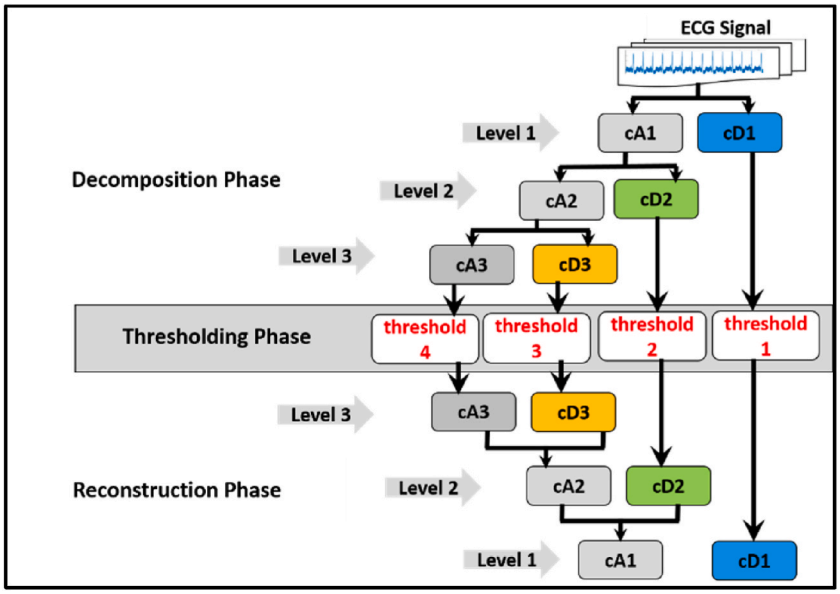


Fig. 1. ECG denoising process.

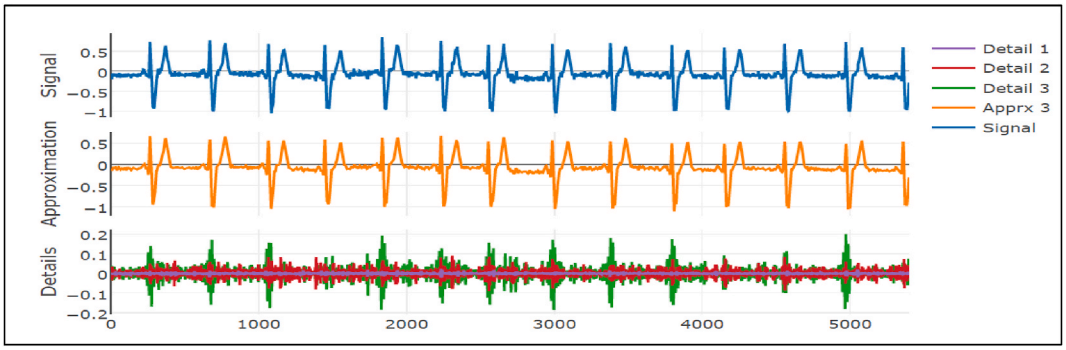


Fig. 2. Details and approximations coefficients.

Where $\sigma = \frac{median\ (|D_{ij}|)}{0.6745}$, D_{ij} are unit-scale detail coefficients, and N is the length of the signal vector.

- **Reconstruction:** The inverse discrete wavelet transform (iDWT) is used to rebuild the ECG denoised signal (Equation (5)) and is explained in Ref. [40].

$$ECG_{denoised} = \sum_{k=-\infty}^{\infty} cA_L(K)\,\phi_i'(t-k) + \sum_{i=1}^{L}\sum_{k=-\infty}^{\infty} cD_{i+1}(K)\psi_i'(t-k) \tag{5}$$

Where 'ECG denoised' is the reconstructed ECG signal and i is the decomposition level. Wavelet denoising comprises five parameters with discrete ranges (Table 1). The effectiveness of noise reduction is determined by the wavelet parameters selected. The three phases of the wavelet denoising procedure are illustrated in Fig. 1. During the first stage, DWT is employed to deconstruct the ECG signal.

The optimal mother wavelet function **(Φ)** is selected for use in this phase's ECG signal decomposition process. The decomposition level **(L)** is typically determined by both the ECG data and prior experience. This paper focuses on optimising WT parameters. In the second phase, thresholding is applied. The wavelet features two typical thresholds **(β)**, namely, hard ***(h)*** and soft ***(s)*** thresholds [50, 52–55]. Fig. 3 illustrates the difference between soft and hard thresholding.

Each type of threshold – ***soft (s) and hard (h)*** – selection rules **(λ)** and rescaling methods **(ρ)** must be selected. These thresholding methods need to be established, as their choice affects the overall performance of noise removal. Typically, the threshold value is determined by the intensity of the noise **(δ)**. Tables 2 and 3 display the various thresholding selection rules and rescaling parameter values.

Lastly, Equation (6) is applied to the thresholding rules.

$$ECG_{noisy}(n) = s(n) + \delta e(n) \tag{6}$$

Here, $s(n)$ represents the clean ECG signal, $e(n)$ represents the noise, δ represents the amplitude of the noise, and n is the sample number. For each wavelet coefficient level ***(cA and cD)***, the parameters **(β, λ, ρ)** must be used independently in order to utilise the wavelet. The iDWT is employed as the final step to reconstruct the ECG signal.

2.2. Particle swarm optimisation

Initially, the use of PSO in optimisation was thoroughly discussed in Ref. [56]. The PSO method begins with several possible solutions, collectively referred to as a swarm. Each solution is represented as a particle, and each particle oscillates repeatedly over the

Table 1
Parameter ranges for wavelet denoising.

Wavelet denoising parameters	Range
Type of wavelet basis function Φ	Coiflet (coif1-coif5), Symlet (sym1-sym45), Daubechies (db1-db45), Fejer-Korovkin (fk4- fk8- fk14- fk18&fk22), and Biorthogonal (bior1.1-bior1.5 & bior2.2-bior2.8 & bior3.1-bior3.9),
Threshold function β	Soft (s), Hard (h)
Level of decomposition L	1–10
Threshold selection of a rule λ	Sqtwolog, Minimax, Heursure, and Rigsure
Rescaling approach ρ	No scaling (one), one level (sln), Several levels (mln).

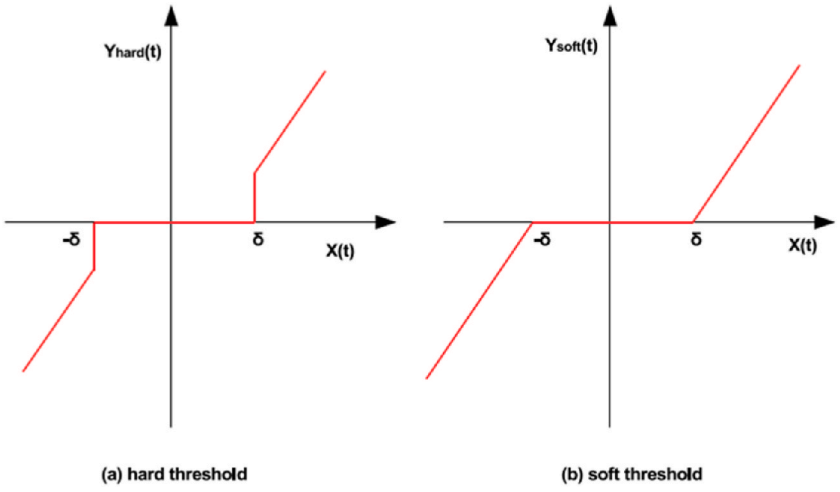


Fig. 3. Hard and soft thresholding techniques.

Table 2
Threshold selection rules.

Threshold selection rule	Description
Rule 1: Rigrsure	The selection of the threshold is based on Stein's Unbiased Risk Estimate (SURE).
Rule 2: Sqtwolog	The threshold is chosen equal to $(\sqrt{2logM}$ where M is number of coefficients in series
Rule 3: Heursure	The threshold is chosen using a combination of the first two rules
Rule 4: Minimaxi	The threshold is chosen to be equal to the Max(MSE)

Table 3
Rescaling methods for wavelet thresholding.

wavelet thresholding rescaling methods ρ	rescaling
sln	Single level
mln	Multiple levels
one	No scaling

search space. With each successive iteration, each particle considers both its locally optimal solution in terms of the fitness function (local best) and the optimal solution among its neighbours (global best). If a particle's performance is gauged by an objective function, then the particle will always be attracted to the optimal solution, both locally and globally. The social behaviour of birds in flocks provides an apt analogy for this process [57]. The PSO code is represented by Algorithm 1. According to this theory, each particle is essentially defined by the following characteristics: (a) $\boldsymbol{x}_i$ is the current location of particle $\boldsymbol{i}$, (b) $\boldsymbol{v}_i$ is the current velocity of particle $\boldsymbol{i}$, (c) $\boldsymbol{y}_i$ is the best local value for particle $\boldsymbol{i}$, and (d) $\widehat{\boldsymbol{y}}_i$ is the best global value for particle $\boldsymbol{i}$. Throughout the enhancement loop (see Algorithm 1, lines 6–16), these four attributes of each particle are updated at every time t.

$$\boldsymbol{y}_i(\boldsymbol{t}+\boldsymbol{1}) = \begin{cases} \boldsymbol{y}_i(\boldsymbol{t}) & \boldsymbol{if}\ \boldsymbol{f}(\boldsymbol{x}_i(\boldsymbol{t}+\boldsymbol{1})) \geq \boldsymbol{f}(\boldsymbol{y}_i(\boldsymbol{t})) \\ \boldsymbol{x}_i(\boldsymbol{t}+\boldsymbol{1}) & \boldsymbol{if}\ \boldsymbol{f}(\boldsymbol{x}_i(\boldsymbol{t}+\boldsymbol{1})) < \boldsymbol{f}(\boldsymbol{y}_i(\boldsymbol{t})) \end{cases} \tag{7}$$

$$\widehat{\boldsymbol{y}} = \{\boldsymbol{y}_i(\boldsymbol{t}) | \boldsymbol{i} = \boldsymbol{arg}_{\boldsymbol{i}=\boldsymbol{1},\ldots,\boldsymbol{N}}\ \boldsymbol{min}\ \boldsymbol{f}(\boldsymbol{y}_i(\boldsymbol{t}))\} \tag{8}$$

Let N represent the number of elements in the swarm. For each dimension's velocity to be updated $j \in [1,Nd]$, according to Equation 9, $v_{i,j}$ is related to the velocity vector from j of particle i. This also incorporates the following elements: $\omega v_{i,j}(t)$ where $v_{i,j}$ is the earlier velocity, and ω regulates the influence of the preceding velocity. The greater the worth of ω, the more anxiety there is with exploration. In comparison, for smaller values of ω, the focus shifts towards exploitation.

$\boldsymbol{y}_{i,j}(\boldsymbol{t}) - \boldsymbol{x}_{i,j}(\boldsymbol{t})$: indicates that particle i is directed towards a local best direction.

$\widehat{\boldsymbol{y}}_j(\boldsymbol{t}) - \boldsymbol{x}_{i,j}(\boldsymbol{t})$: indicates that a particle i is directed to a global best direction.

$$\boldsymbol{v}_i(\boldsymbol{t}+\boldsymbol{1}) = \boldsymbol{\omega}\boldsymbol{v}_{i,j}(\boldsymbol{t}) + \boldsymbol{c_1}\boldsymbol{r_{1,j}}(\boldsymbol{t})\left(\boldsymbol{y}_{i,j}(\boldsymbol{t}) - \boldsymbol{x}_{i,j}(\boldsymbol{t})\right) + \boldsymbol{c_2}\boldsymbol{r_{2,j}}(\boldsymbol{t})\ \left(\widehat{\boldsymbol{y}}_j(\boldsymbol{t}) - \boldsymbol{x}_{i,j}(\boldsymbol{t})\right) \tag{9}$$

Where ω is called the 'intra-weight', which controls the historical velocity, c_1 and c_2 are two acceleration constants, and r_1 and r_2 generate a uniformly distributed random number between 0 and 1. Equation 8 updates the current position of particle i.

$$x_i(t+1) = x_i(t) + v_i(t+1) \tag{10}$$

Algorithm 1. PSO

```
for i = 1, …, N do
        x_i = Generate_Initital Position for Particle (i)
        v_i = 0
        v_i = x_i
end for
repeat
for i = 1, …, N do
        f (i) = Evaluate Particle (i)
        y_i = Update Using Equation (7)
        ŷi = Update Using Equation (8)
        for j = 1, …, Nd do
                v_i = Update Velocity Using Equation (9)
        end for
        x_i = Update Using Equation (10)
end for
until (Stopping Criteria is met)
```

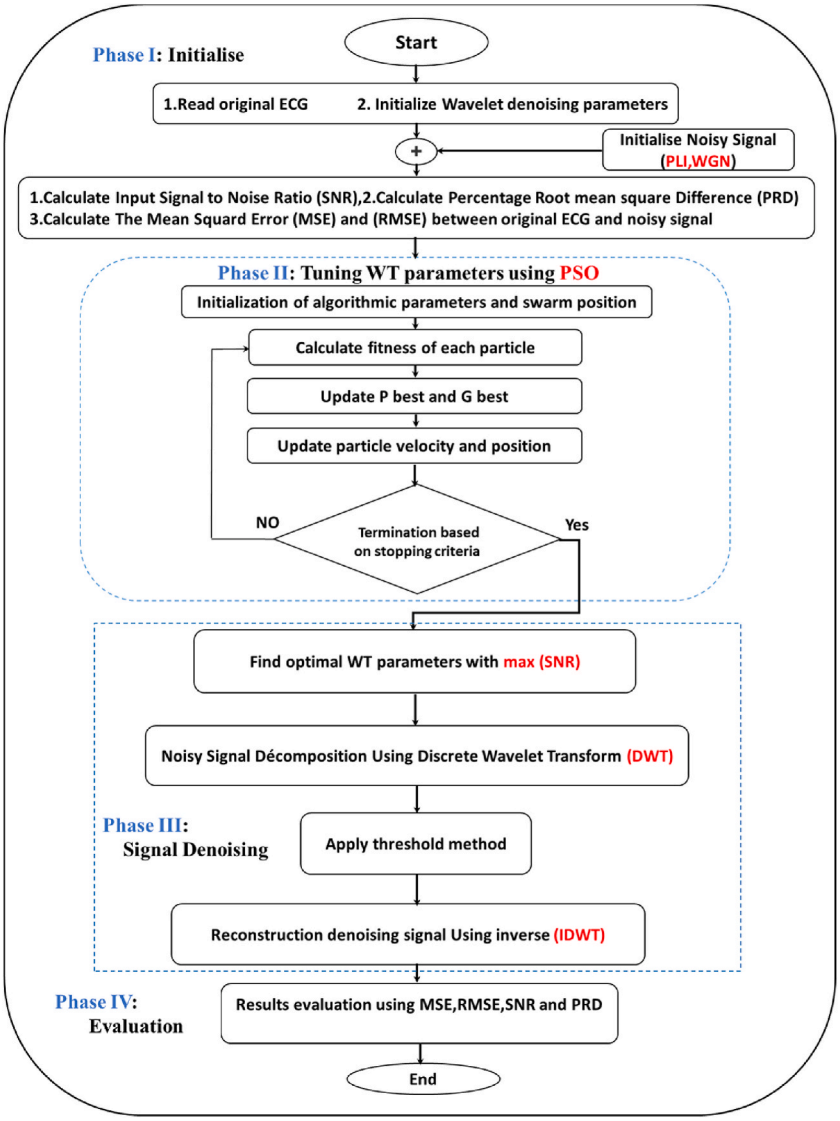


Fig. 4. Proposed method.

3. Proposed PSO and WT for ECG signal denoising

This section provides a comprehensive analysis of the suggested approach, combining PSO with WT (PSO-WT) to denoise ECG signals. Consider that ECG signals are distorted by noise, which is a potential cause of the issue. The best wavelet denoising parameters for the ECG signal have been determined using PSO. As shown in Fig. 4, the proposed PSO-WT denoising technique can be described as follows:

Input: A noisy ECG signal and parameters for wavelet denoising (Φ, L, β, λ, ρ).

Processing:

a. Set appropriate ranges for wavelet thresholding denoising parameters of the ECG signal and construct objective functions with SNR.
b. Use PSO to optimise wavelet denoising parameters, selecting the optimal parameters based on noise suppression performance.
c. Perform a WT on the noisy ECG signal to obtain all wavelet coefficients.
d. Apply optimal thresholds to the noisy coefficients within the ECG signal to acquire modified ECG components.

Output: Reconstruct the denoised ECG signal.

The proposed method can then be summarised in Algorithm 2.

Algorithm 2. Applying PSO Algorithms to Tune WT Parameters for ECG Signal Denoising

1: Initialise noisy ECG signal (nECG), and calculate the SNR, MSE, RMSE, and PRD for input ECG signal.
2: Initialise PSO operators, initialise solution(s)
X_i (i = 1, 2, … Np) Np = 5 wavelet parameters,
The initial solution X_i (Φ, L, β, λ, ρ)
3: $X'opt$ = PSO (X, X_i)
4: ECG Denoised = WT ($X'opt$, nECG)
5: ECG Out Signals = Evaluate (ECG Denoised, SNRout, SNRimp, MSE, RMSE, PRD).

The phases below show a detailed explanation of the proposed method:

Phase I. Initialisation. This phase includes three steps. The first step is to read the input ECG signal $S(n)$ from the source. The WT denoising method was developed because the original ECG signal was corrupted by WGN using equation (11) and PLI using equation (12). These noises mimic disturbances that may contaminate the original ECG signal during recording. These forms of interference serve as a data set for evaluating the efficacy of the suggested approach.

$$\boldsymbol{N(t) = s(t) + \sigma} \tag{11}$$

$$\boldsymbol{N(t) = A\ sin\ (2\pi ft)} \tag{12}$$

The second step of this phase is to initialise the WT denoising parameters (Φ, L, β, λ, ρ) from the ranges given in Table 1. The PSO parameters are set as follows: $C_1 = 2$, $C_2 = 2$, $N_P = 5$, $itermax = 50$, $pop_size = 100$. C_1 and C_2 are the acceleration constants, N_p is the number of WT parameters, *itermax* is the maximum number of iterations, and *pop_size* is the population size. Finally, calculate the SNR using equations (13)–(15), PRD using equation (25), MSE by equation (23), and root MSE (RMSE) according to equation (24). Electrocardiogram signal data will be recorded both before and after the denoising operation.

Phase II. PSO-based parameter tuning of WT. The proposed method uses PSO to find the optimal WT parameters for denoising the

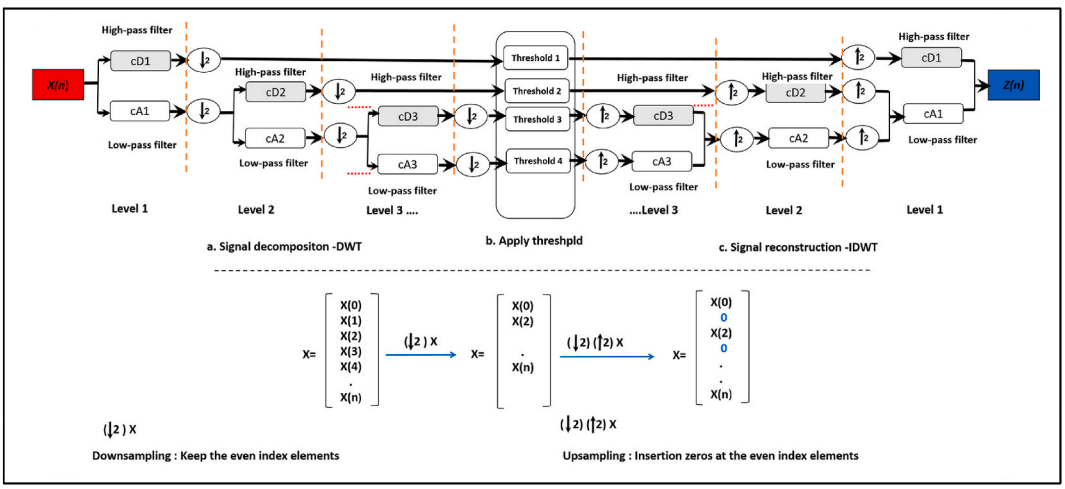


Fig. 5. ECG denoising procedure.

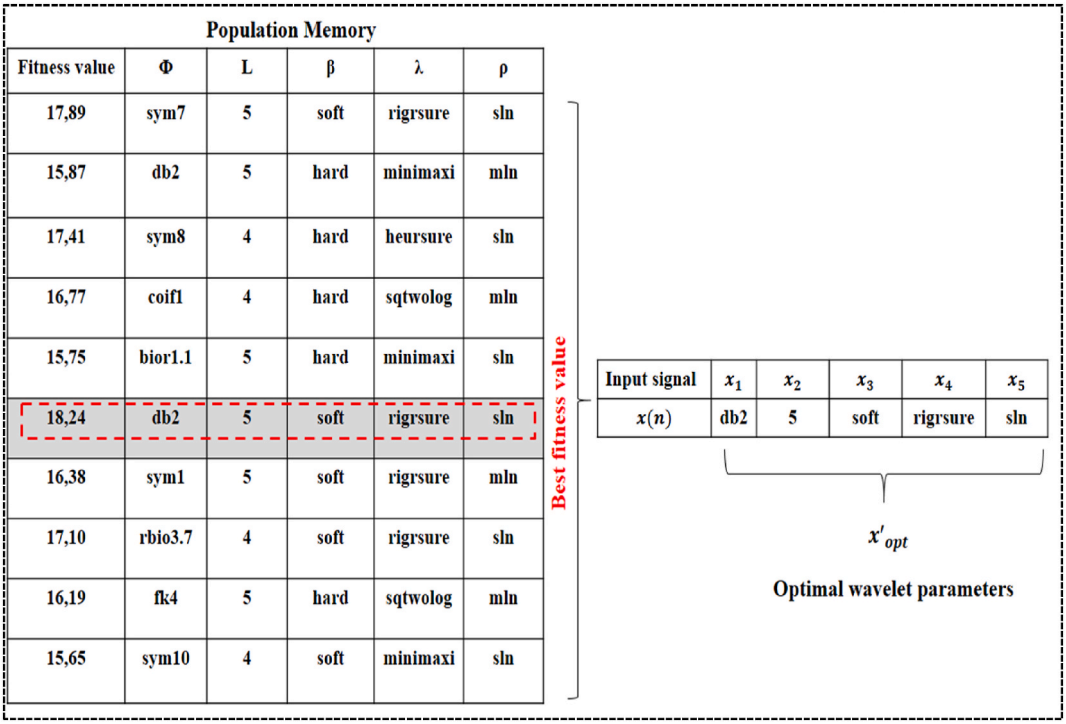


Fig. 6. PSO-optimal WT parameter selection for ECG signal noise removal.

ECG signal. Initially, the configuration of the WT parameters is represented as a vector $x = (x_1, x_2, \ldots, x_n)$, where n is the number of WT parameters equal to 5. Here, x_1 shows the parameter value of the mother WT function Φ; x_2 represents the value of the level of decomposition parameter L; x_3 is the method for setting a threshold β; x_4 indicates the thresholding selection rule of the parameter value λ; and x_5 is the rescaling method being used ρ, where the range for these parameter values is chosen from Table 1. Fig. 6 provides an example of a WT parameter solution for ECG signal denoising. The objective function SNR is employed by the PSO algorithm to evaluate the result, which is defined as follows:

$$SNR_{imp} = SNR_{output} - SNR_{input} \tag{13}$$

Where SNR_{input} and SNR_{output} are as follows:

$$SNR_{input} = 10\, log_{10} \frac{\sum_{n=1}^{N} [S(n)]^2}{\sum_{n=1}^{N} [S(n) - \widetilde{S}(n))]^2} \tag{14}$$

$$SNR_{output} = 10\, log_{10} \frac{\sum_{n=1}^{N} [S(n)]^2}{\sum_{n=1}^{N} [S(n) - \widehat{S}(n))]^2} \tag{15}$$

Here $S(n)$ represents the original ECG signal; $\widetilde{S}(n)$ is the noisy ECG signal; and $\widehat{S}(n)$ is the denoised ECG signal generated by tweaking wavelet parameters using the PSO algorithm. Iteratively, refines the randomly generated solution. The output from this phase is an optimised solution $x'_{opt} = (x'_1, x'_2, .., x'_n)$ that will be sent on to the next phase.

Phase III. ECG noise removal with WT. Dependent on x'_{opt}, the denoising process of WT consists of three primary phases, as shown in Fig. 1 and explained in further detail below:

- **Decomposition of ECG signals using DWT:** During this phase, the DWT decomposes the noise in the input ECG signal ,$S(n)$. The first and second x'_{opt} parameters (mother wavelet Φ and the level of decomposition L) must be employed in the procedure for decomposition. Fig. 5 illustrates the DWT technique for three levels, where each level separates the noisy ECG data into cA and cD. In the next step, the latter is treated with a high-pass filter, whereas the former is broken down and treated with a low-pass filter. Using low-pass and high-pass filters, the ECG signal is convolved. The down-sampling operator, represented by block (↓2), is used

to keep the even indicator components of the ECG signal according to their frequency and frequency intensity, *cA* and *cD* are extracted from the ECG signal.

- **Thresholding:** It is the second phase of ECG denoising, which depends on the coefficient of the noise level. In this phase, thresholding type (β), thresholding selection criteria (λ), and rescaling techniques (ρ) must be chosen from x'_{opt}. By applying a thresholding technique (Equation (16)) to the noisy and non-stationary signal $\widehat{X}$, we can evaluate the denoising of the ECG signal, according to Ref. [21], as follows:

$$\boldsymbol{Z} = \boldsymbol{THR}(\widehat{\boldsymbol{X}}, \boldsymbol{\delta}) \tag{16}$$

Where THR represents the function of thresholding, and δ represents the value of the threshold. The performance of ECG noise removal in the wavelet domain depends on the estimate of δ. Hence, several approaches for estimating have been offered. Donoho and Johnstone [51] determined the threshold in Equation (17):

$$\boldsymbol{\delta} = \boldsymbol{\sigma}\sqrt{\boldsymbol{2logM}} \tag{17}$$

Where σ is the standard deviation of the DWT coefficients, and M is their length vector.

We estimate the threshold value as follows, given that it only depends on *cD* and *cA* has the lowest frequency and most energy of all the ECG signals, according to the level of the coefficients, as indicated in Equation (18):

$$\widehat{x}_d(l) = THR(\widehat{x}_d(l),\ \delta_l), l = 1, 2, \ldots \tag{18}$$

Where $\widehat{x}_d$ denotes the vector of DWT threshold detailed coefficients, l refers to the WT decomposition level, and δ_l is a threshold value set for such a level. As seen earlier, Fig. 3 demonstrates that the wavelet typically provides two different types of thresholding-specific functions (β), namely, soft and hard thresholding.

Below are descriptions of the distinctions between hard and soft thresholding, As indicated in Equations (19) and (20), respectively:

$$\widehat{x}_{di}(l) = \begin{cases} \widehat{x}_{di}(l) - \ |\delta_l| & |\widehat{x}_{di}(l)| \geq \delta_l \\ 0 & |\widehat{x}_{di}(l)| < \delta_l \end{cases} \tag{19}$$

$$\widehat{x}_{di}(l) = \begin{cases} \widehat{x}_{di}(l) & |\widehat{x}_{di}(l)| \geq \delta_l \\ 0 & |\widehat{x}_{di}(l)| < \delta_l \end{cases} \tag{20}$$

Where i is the DWT detailed coefficient index at a level l. Equation (21) summarizes the thresholding DWT coefficients.

$$\widehat{X} = [\widehat{x}_d(1) \quad \widehat{x}_d(2) \quad \widehat{x}_a(2)] \tag{21}$$

- **iDWT reconstruction of the denoised ECG signal:** Using iDWT on $\widehat{X}$, we calculate the original ECG signal using Equation (22) as follows:

$$z[n] = \sum\nolimits_{k=-\infty}^{\infty} cA_L(K)\ \Phi'_i(n-k) + \sum\nolimits_{i=1}^{L} \sum_{k=-\infty}^{\infty} cD_{i+1}(K)\Psi'_i(n-k) \tag{22}$$

The ECG is convolved via up-sampling (↑2), which entails inserting zeros at the even index components of the ECG signals. As an example, Fig. 5 depicts the iDWT technique for three levels.

Phase IV. ECG denoising evaluation in the last phase. The ECG results produced using WT are evaluated. The evaluation will be conducted using the following criteria: SNR, SNR improvement, MSE as per equation (23), RMSE as per equation (24), and PRD as per equation (25).

$$MSE = \frac{1}{N}\sum_{n=1}^{N}(S(n) - \widehat{S}(n))^2 \tag{23}$$

$$RMSE = \sqrt{\sum_{n=1}^{N}\frac{1}{N}[S(n) - \widehat{S}(n))]^2} \tag{24}$$

$$PRD = 100^* \sqrt{\frac{\sum_{n=1}^{N}[S(n) - \widehat{S}(n))]^2}{\sum_{n=1}^{N}[S(n)]^2}} \tag{25}$$

where $S(n)$ represents the original ECG signal, $\widetilde{S}(n)$ is the noisy ECG signal, and $\widehat{S}(n)$ is the denoised ECG signal generated through the

tweaking of the WT parameters by using the specified PSO method, and N is the sample number.

4. Results and discussions

To evaluate the efficiency of filtration in the proposed method, we downloaded several records from the well-known and publicly available MIT-BIH database [58]. Each ECG record has the following characteristics: a 650,000-sample length, a 360 Hz sampling rate, an 11-bit resolution across a 10 mV range, and a 3960 bps bit rate. This database is frequently used as a benchmark for comparing various noise-removal methods in the literature.

In this work, we introduced two types of noise to clean ECG signals: WGN and PLI. These parameters were selected experimentally to optimise their settings. PSO was proposed to obtain an optimal set of parameters for effective noise reduction. Table 1 displays the parameters to be optimised.

In this work, the parameters for wavelet noise removal were optimised using MATLAB 2018b software. The parameters utilised for PSO analysis are as follows: $C_1 = 2$, $C_2 = 2$, $N_P = 5$, $itermax = 50$, and $pop_size = 100$. The stopping point was determined based on convergence tolerance for fitness.

4.1. WGN removal

The optimised parameters for wavelet denoising, derived by the PSO, are presented in Table 4. Usually, it is not guaranteed that noise can be efficiently removed using a single wavelet. We found that some wavelets achieved better noise removal than others. The orthogonal WTs, such as Coiflets and Symlets, offer several advantages. They are extremely brief and allow for flawless and straightforward reproduction of the original signal [59]. Based on the results obtained, the Coiflets family is more appropriate for ECGs contaminated by high noise levels, while the Symlets family is more suitable for ECGs contaminated by low noise levels. Due to the relationship between level decomposition and noise level, the appropriate decomposition level for a high noise level is 7–8, while for a low noise level, it is 3–4. Even though the hard threshold is simpler than the soft threshold, the latter can yield better results. Among the three thresholding rescaling techniques, the 'sln' technique performed the best. Additionally, the 'rigrsure' technique was found to be more efficient. In this study, we conducted experiments using 16 ECG records obtained from the MIT-BIH database to determine the optimal wavelet denoising parameters achieved by PSO, with SNR improvement as a fitness function.

After filtration, the average SNR, PRD, MSE, and RMSE values are obtained for the signal. Table 5 displays the ECG signal results, denoised using the PSO-WT denoising technique. For SNR_{input}, values varied from −5 dB to 30 dB with a step of 5 dB. Fig. 7 depicts an example of the obtained result, record number 100, from the MIT-BIH database. It represents the original (Fig. 7-a), noisy (Fig. 7-b), and denoised signals (Fig. 7-c) produced using the proposed method. It can be clearly seen that the denoised signal is very close to the original ECG, which proves the effectiveness of the proposed method.

Furthermore, the proposed approach yields results corresponding to a noisy signal with a SNR_{input} of 10 dB, a PRD of 13.47 and an output SNR of 18.24. A significant improvement of 8.24 in SNR is achieved. Fig. 8(a) depicts the relationship as a function of the input and output SNR. The relationship between them is almost linear; they are directly proportional. When the SNR_{input} increases, the SNR_{output} also increases. Fig. 8(b) shows a graphical representation of the PRD between the original and the denoised ECG signal, with detailed values in Table 5. Fig. 8(b) shows that the proposed approach is smoothest when there is less noise. Note that a lower PRD implies efficient signal denoising. Fig. 8(c) and (e) show the MSE and RMSE between the original and the denoised ECG signals. We note that the MSE and RMSE values are inversely proportional to the SNR_{input} values.

The improvement in the SNR obtained by our proposed method is identified as the difference between the SNR_{output} (dB) and the SNR_{input} (dB), allowing us to evaluate the noise elimination performance. The relationship between the SNR improvement and the SNR_{input} is shown in Fig. 8(d). It is clear that improvements in SNR are greater when the SNR_{input} levels are low. Consequently, our proposed method performs well when significant noise levels are present.

A thorough comparison of the improvements in SNR and PRD, obtained using our proposed denoising technique, is made against more than 10 other state-of-the-art noise-removal techniques [60] using the same database. All these comparisons are shown in Fig. 9. As the reported results from the literature come from different values of input SNR applied to different records from the MIT-BIH database, we have divided our comparisons according to the SNR_{input} values and the ECG records used as reported by counterpart techniques. Therefore, a comparison based on four values of SNR_{input} (−5, 0, 5, and 10) using record 100 is made against the following techniques: EMD with an NLM (EMD-NLM) [29], conventional filtering (CF) [30], and NLM denoising of ECG signals (NLM) [31]. Fig. 9(a) and (b) depict this comparison. A comparison based on three values of SNR_{input} (−5, 0, and 5) using record 103 is made

Table 4
The optimal WT denoising parameters were found by the PSO for the signal being tested.

WT denoising parameters	SNR input values		
	SNR in <10 dB	10 dB < SNR in <25 dB	SNR in >25 dB
The type of wavelet basis function φ	Coif 3	Sym 3	Sym 18
Thresholding function β	soft	soft	soft
Decomposition level L	8,7	6,5	4,3
Thresholding selection rule λ	rigsure	rigsure	rigsure
Rescaling approach ρ	sln	sln	sln

Table 5
The effectiveness of denoising ECG signals at different levels of input SNR.

Input SNR (dB)	Output SNR (dB)	Improvement SNR (dB)	MSE	RMSE	PRD %
−5	7.5034	12.5740	0.0759	0.2550	50.5431
0	10.7463	10.8169	0.0342	0.1701	31.6505
5	14.5189	9.5895	0.0143	0.1103	20.1725
10	18.4955	8.5661	0.0059	0.0708	12.8114
15	22.3989	7 .4695	0.0024	0.0448	8.1116
20	26.1904	6 .2610	0.0009	0.0287	5.2273
25	29.8667	4.9373	0.0004	0.0184	3.3552
30	33.5884	3.5416	0.0002	0.0121	2.2019

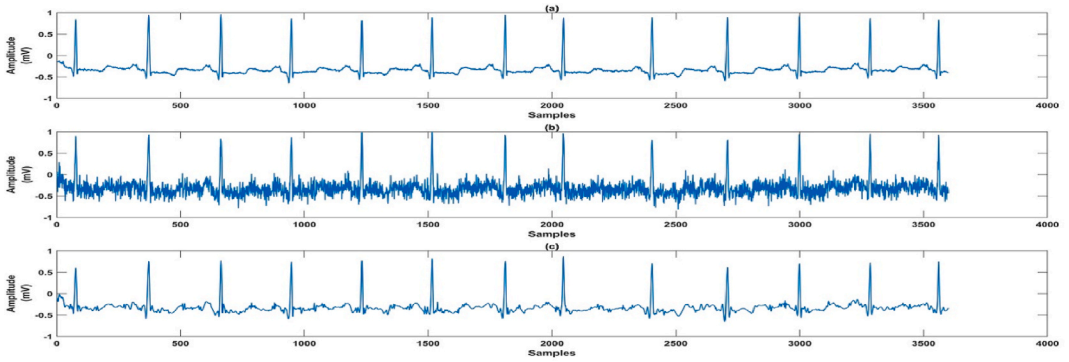


Fig. 7. (a) The clean ECG signal (one sample as an illustration), (b) the corrupted ECG signal with noise at $SNR_{input} = 10$ dB, (c) the denoised ECG signal resulting from the proposed technique (φ = sym3, β = soft, λ = rigsure, $L = 5$, and ρ = sln) with $SNR_{output} = 18.24$ dB.

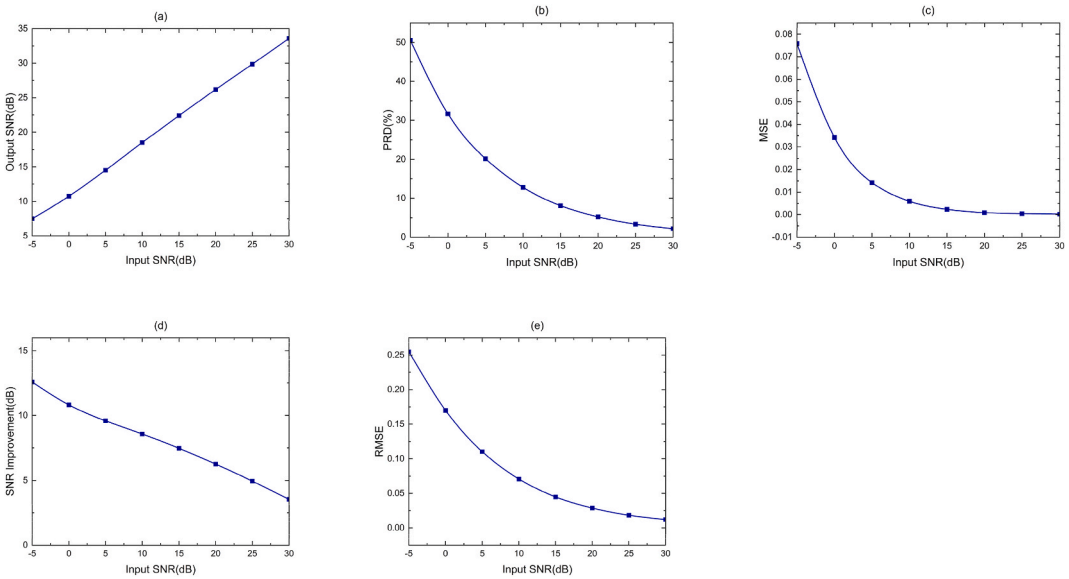


Fig. 8. (a) The dependence of SNR_{output} with the SNR_{input}, (b) PRD with SNR_{input}, (c) MSE with the SNR_{input}, (d) SNR Improvement with the SNR_{input}, and (e) RMSE with the SNR_{input}.

against the IHP-ST EMD [32] and SF [33] methods, as shown in Fig. 9(c) and (d). Another comparison based on two values of SNR_{input} (5 and 10) using records 100 and 103 is made against the following techniques: EMD-ASMF [34], SDCST [35], NIWT [36], 1DTVD [37], and GAMNVE [38], as shown in Fig. 9(e)-(f), Fig. 9(g), and Fig. 9(h), respectively. It can be clearly seen from Fig. 9 that our proposed technique outperforms all other state-of-the-art techniques for all SNR_{input} levels in terms of improvements in SNR and provides the lowest value in PRD. Therefore, the proposed PSO has succeeded in optimising the parameters for wavelet denoising of ECG signals, resulting in higher performance than state-of-the-art techniques. In addition, it can be observed that the acquired SNR

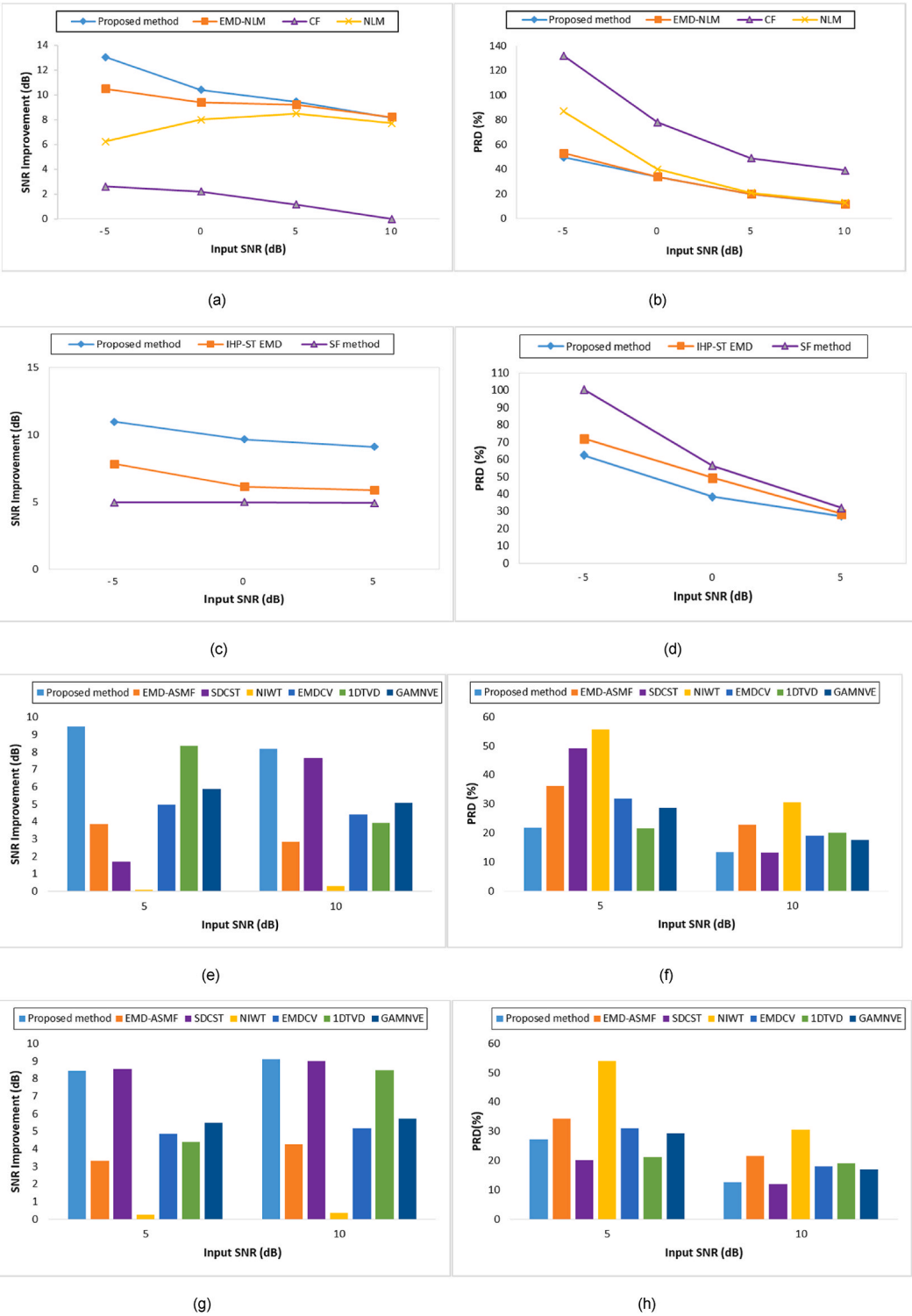


Fig. 9. The improvement SNR and PRD for several denoising techniques.

improvements for the ECG signal are vulnerable to high amounts of noise.

4.2. PLI removal

The proposed technique was also tested on the second type of additive noise: PLI. This noise was added to the generated ECG signal from the MIT-BIH database with two fundamental frequencies, 50 Hz and 60 Hz. The experiment was conducted on 16 different samples from this database, where the average of the SNR_{output} was calculated. For instance, Fig. 10 depicts an example of the application of our proposed method on record number 100 from the MIT-BIH database. The original, noisy, and denoised signals are shown, respectively, in Fig. 10(a), (b), and 10(c). It is evident that the denoised signal closely resembles the original ECG signal. Furthermore, a SNR_{output} of 22.69 dB is obtained for a SNR_{input} of 10 dB at frequency $f = 50$ Hz. This represents a significant SNR improvement of 12.69, further affirming the effectiveness of the proposed method.

In Tables 6 and 7, the SNR_{output} obtained from our denoising method (PSO-WT) is compared with other published noise removal methods, namely EVD-based technique [28], MRLS-based technique [24], and EMD-WT-based technique [27] for the removal of PLI noise. It is clear from the tables that our proposed method outperforms the other techniques mentioned. Values highlighted in bold correspond to the best values for each SNR level and each ECG record. However, as seen in Table 6, the MRLS approach performed best at low noise levels for the 50 Hz frequency, but our method outperformed it at higher noise levels. It is also noteworthy that the EMD-EWT-based technique [26] outperformed the proposed method in most cases at this frequency. Another key point is that the proposed approach showed excellent results and outperformed all other state-of-the-art techniques for noise elimination at a frequency of 60 Hz, as shown in Table 7. Overall, the results substantiate the effectiveness of our method in comparison to other state-of-the-art methods in removing this type of noise.

The results presented in Tables 6 and 7 are summarised in Fig. 11 using box-plot diagrams. The findings in Fig. 11(a) show that, in the case of a 50 Hz frequency, the EMD-EWT method offers the best SNR_{output} with a maximum of 35 dB and an average of 26 dB. In this instance, the proposed method delivers an acceptable level of SNR_{output}, where the average is around 21 dB. In the case of $f = 60$Hz Fig. 11(b), the proposed method exhibits the best performance with an average of 28 dB, compared to an SNR_{output} of 27 dB for the EMD-EWT method. In the latter case, most of the tests conducted with the proposed method yielded an SNR_{output} greater than 25 dB.

To showcase the efficacy of the proposed approach, we conducted a comparative analysis against results obtained through similar methodologies presented in prior works. In Ref. [61], the authors introduce an innovative ECG signal denoising method that combines genetic algorithm (GA) and wavelet transformation (WT). Table 8 comprehensively compares key metrics between our approach and the outcomes detailed in Ref. [61]. The results unequivocally demonstrate the superiority of the PSO-WT method over the GA-WT method in the removal of Power Line Interference (PLI) at a frequency of 50Hz from various ECG signals, considering different input SNR values. Specifically, the PSO-WT method consistently yields higher SNR values and lower values for MSE, RMSE, and PRD, signifying its ability to preserve the quality and integrity of the original ECG signals while effectively mitigating interference.

5. Conclusion

This paper presents a combined technique between particle swarm optimisation (PSO) and wavelet transform (WT) for ECG noise removal. In the proposed method, two main noises are added to the clean ECG signal to simulate what the ECG signal is exposed to during recording time. The first noise is a white Gaussian noise, and the second is a power line interference noise, which is added at two different fundamental frequencies, 50 Hz and 60 Hz. The proposed method is used as a pre-processing approach to remove ECG noise for further analysis and classification.

The success of any WT-based ECG signal denoising process is closely related to the wavelet noise reduction parameters. Therefore, this work presents the PSO algorithm as a method for optimising complete wavelet noise reduction parameters to effectively filter the ECG signal. Based on the PSO algorithm, we have reached the best solution, which corresponds to the best fitness function of five optimised parameters: type of wavelet basis function Φ, thresholding function β, decomposition level L, threshold selection rule λ and rescaling method ρ.

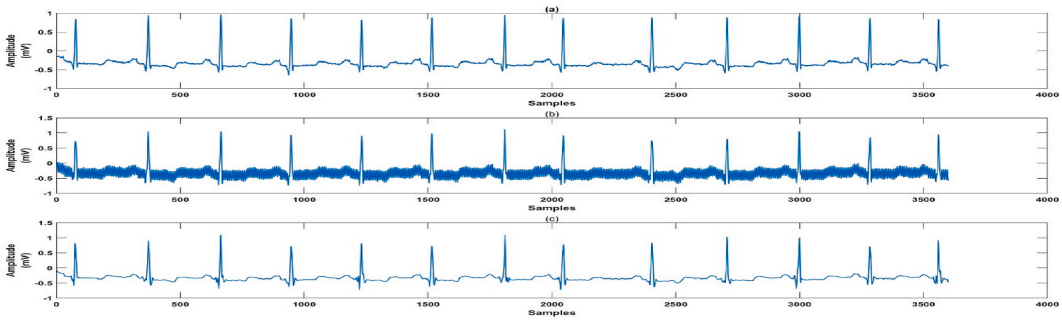


Fig. 10. (a) Clean ECG, (b) the corrupted ECG signal with noise at $SNR_{input} = 10$ dB, (c) the denoised ECG signal resulting from the proposed technique ($\varphi =$ db2, $\beta =$ hard, $\lambda =$ rigsure, $L = 3$, and $\rho =$ mln).

Table 6
Comparison of PLI removal ($f = 50Hz$) from various ECG signals at varying SNR_{input} values, compared in terms of SNR_{output} as averaged values over 20 segments.

ECG Record	$SNR_{inp} = -10$ dB					$SNR_{inp} = -5$ dB					$SNR_{inp} = 0$ dB				
	SNR_{out}(dB)														
	Proposed	EVD [28]	MRLS [24]	EMD-WT [27]	EMD-EWT [26]	**Proposed**	EVD [28]	MRLS [24]	EMD-WT [27]	EMD-EWT [26]	**Proposed**	EVD [28]	MRLS [24]	EMD-WT [27]	EMD-EWT [26]
100 m	14.065	3.758	13.666	11.366	**18.985**	16.322	7.284	17.899	11.869	**21.809**	16.198	11.683	21.583	11.547	**23.057**
102 m	13.626	3.770	13.560	13.958	**18.934**	14.913	7.462	17.651	14.926	**21.858**	15.582	10.526	21.161	15.716	**23.561**
103 m	13.455	3.770	13.984	13.804	**20.272**	14.580	7.300	18.472	15.313	**24.602**	17.055	11.707	22.815	16.294	**27.885**
105 m	**21.418**	3.772	14.054	19.238	20.378	22.887	7.302	18.625	21.846	**25.038**	23.586	11.711	23.116	24.422	**29.222**
109 m	**23.054**	3.773	14.095	20.012	20.424	24.889	7.305	18.590	23.420	**25.198**	25.771	7.420	23.023	25.503	**29.605**
116 m	17.638	3.775	14.122	15.267	**20.202**	18.221	7.307	18.547	17.759	**24.655**	18.450	11.718	22.719	18.515	**28.222**
119 m	**20.436**	3.774	14.071	17.066	20.362	21.718	7.305	18.481	19.252	**25.029**	22.530	11.716	22.797	21.013	**29.128**
123 m	**20.827**	3.769	14.056	13.270	20.249	21.884	7.114	18.635	15.344	**24.737**	22.279	10.867	23.092	16.156	**27.963**
201 m	18.289	3.770	13.789	16.956	**20.276**	19.046	7.299	18.268	19.434	**24.864**	19.314	11.706	22.497	20.428	**28.793**
205 m	16.033	3.779	13.691	12.754	**20.074**	16.246	7.312	18.068	13.260	**24.210**	17.255	11.723	22.117	14.811	**26.787**
213 m	16.597	3.772	14.146	18.008	**20.431**	17.135	7.303	18.601	21.485	**25.092**	17.372	4.681	22.911	23.389	**29.352**
219 m	19.923	3.768	14.069	17.622	**20.298**	20.754	7.626	18.500	19.643	**24.910**	21.165	11.885	22.800	21.540	**28.939**
220 m	14.574	3.775	13.955	11.075	**19.623**	15.419	7.308	18.357	11.919	**23.006**	17.281	11.721	22.396	11.216	**24.495**
221 m	16.244	3.770	13.971	16.442	**20.280**	16.634	7.301	18.463	18.355	**24.863**	16.779	11.711	22.798	19.619	**28.827**
223 m	**20.933**	3.767	14.048	18.023	20.383	22.002	7.296	18.513	19.867	**25.076**	22.278	11.702	22.862	21.894	**29.335**
231 m	10.470	3.767	13.946	11.604	**20.134**	12.986	7.295	18.409	13.221	**24.162**	16.542	11.405	22.619	13.154	**26.302**
AVG	17.349	3.770	13.951	15.404	**20.082**	18.477	7.320	18.380	17.307	**24.319**	19.340	10.868	22.582	18.451	**27.592**

ECG Record	$SNR_{inp} = 5$ dB					$SNR_{inp} = 10$ dB				
	SNR_{out}(dB)									
	Proposed	EVD [28]	MRLS [24]	EMD-WT [27]	EMD-EWT [26]	**Proposed**	EVD [28]	MRLS [24]	EMD-WT [27]	EMD-EWT [26]
100 m	19.740	16.045	23.931	11.458	**23.700**	22.487	18.872	**25.648**	14.349	24.944
102 m	18.113	5.480	23.714	16.125	**25.164**	20.691	2.371	25.756	17.313	**27.353**
103 m	20.933	15.314	26.680	14.873	**29.042**	23.953	9.675	29.781	15.335	**30.179**
105 m	24.134	13.795	27.219	24.887	**32.356**	25.109	5.800	30.749	25.856	**34.112**
109 m	26.062	5.251	27.205	26.972	**33.232**	26.143	4.407	30.962	27.390	**35.536**
116 m	20.297	11.099	26.458	19.558	**30.065**	24.551	6.060	29.476	18.903	**30.385**
119 m	23.513	15.167	26.891	21.544	**31.859**	26.509	9.161	30.242	20.212	**32.610**
123 m	23.027	15.131	27.054	13.747	**28.451**	27.023	15.784	**29.406**	17.211	28.360
201 m	21.023	16.200	26.299	21.258	**31.390**	23.727	15.491	29.620	20.444	**32.479**
205 m	20.134	16.524	25.706	12.038	**26.655**	23.898	13.542	**28.065**	14.717	26.835
213 m	19.503	4.390	26.962	24.891	**32.706**	22.875	3.860	30.679	25.093	**34.745**
219 m	21.496	11.099	26.812	22.216	**31.759**	23.855	8.261	30.433	21.338	**32.787**
220 m	20.914	15.813	24.963	11.081	**23.440**	24.245	10.436	**25.868**	15.084	25.222
221 m	20.863	15.311	26.670	20.072	**31.415**	23.452	12.536	29.911	18.821	**32.473**
223 m	22.552	11.401	26.839	22.453	**32.448**	26.206	3.946	30.370	22.054	**33.760**
231 m	20.044	11.336	26.044	12.883	**25.333**	23.128	6.254	**27.780**	16.877	26.780
AVG	21.397	12.460	26.215	18.503	**29.314**	24.245	9.153	29.047	19.437	**30.535**

Table 7
Comparison of PLI removal ($f = 60Hz$) from various ECG signals at varying SNR_{input} values, compared in terms of SNR_{output} as averaged values over 20 segments.

ECG Record	$SNR_{inp} = -10$ dB					$SNR_{inp} = -5$ dB					$SNR_{inp} = 0$ dB				
	SNR_{out}(dB)														
	Proposed	EVD [28]	MRLS [24]	EMD-WT [27]	EMD-EWT [26]	**Proposed**	EVD [28]	MRLS [24]	EMD-WT [27]	EMD-EWT [26]	**Proposed**	EVD [28]	MRLS [24]	EMD-WT [27]	EMD-EWT [26]
100 m	**23.057**	3.754	11.310	13.932	18.682	**25.353**	7.251	15.866	14.924	22.260	**26.566**	11.582	20.184	16.220	24.476
102 m	**19.281**	3.750	11.269	15.456	18.283	20.313	7.420	15.752	16.373	**21.535**	20.750	10.436	19.892	17.553	**23.381**
103 m	**24.567**	3.761	11.321	16.383	19.097	**27.494**	7.304	15.992	19.819	23.426	**29.036**	11.727	20.633	20.540	26.839
105 m	**21.863**	3.761	11.432	21.702	19.310	**25.831**	7.276	16.179	24.234	23.860	**28.623**	11.650	20.962	25.481	27.729
109 m	**24.414**	3.766	11.429	22.358	19.424	**27.965**	7.292	16.209	25.485	24.141	**30.488**	8.450	21.043	27.256	28.446
116 m	**24.364**	3.766	11.482	18.295	19.411	**28.157**	7.294	16.302	20.732	24.161	**30.665**	11.697	21.234	21.918	28.522
119 m	**24.708**	3.771	11.467	20.128	19.487	**29.180**	7.302	16.296	22.138	24.349	**32.837**	11.712	21.235	24.462	28.995
123 m	**24.862**	3.771	11.372	16.818	19.444	**29.597**	7.117	16.110	18.570	24.208	**33.769**	10.870	20.961	20.582	28.583
201 m	**24.212**	3.764	11.369	19.663	19.126	**27.181**	7.285	16.012	21.069	23.329	**28.858**	11.663	20.607	23.495	26.555
205 m	**24.227**	3.771	11.399	16.870	19.402	**28.279**	7.301	16.112	18.047	24.128	**31.128**	11.710	20.928	19.106	28.246
213 m	**24.828**	3.770	11.445	21.348	19.520	**29.043**	7.300	16.264	23.809	24.467	**32.183**	4.678	21.226	27.507	29.369
219 m	**24.686**	3.770	11.436	20.393	19.486	**28.879**	7.632	16.254	22.095	24.320	**31.967**	11.891	21.193	24.485	28.915
220 m	**24.010**	3.768	11.373	14.297	19.180	**27.494**	7.298	16.058	15.656	23.584	**29.578**	11.705	20.703	17.526	27.225
221 m	**23.760**	3.765	11.347	19.177	19.087	**26.387**	7.280	15.991	20.644	23.200	**27.675**	11.644	20.518	22.693	26.279
223 m	**25.127**	3.769	11.444	20.709	19.498	**29.575**	7.299	16.251	22.598	24.387	**33.072**	11.706	21.164	24.998	29.166
231 m	**23.815**	3.772	11.419	14.741	19.286	**26.223**	7.304	16.174	17.290	23.920	27.414	11.421	21.023	19.209	**27.880**
AVG	**23.861**	3.765	11.395	18.267	19.233	**27.309**	7.310	16.114	20.218	23.705	**29.663**	10.909	20.844	22.064	27.538

ECG Record	$SNR_{inp} = 5$ dB					$SNR_{inp} = 10$ dB				
	SNR_{out}(dB)									
	Proposed	EVD [28]	MRLS [24]	EMD-WT [27]	EMD-EWT [26]	**Proposed**	EVD [28]	MRLS [24]	EMD-WT [27]	EMD-EWT [26]
100 m	**27.113**	15.785	23.297	17.781	**25.407**	**27.477**	18.767	24.895	18.549	26.002
102 m	21.015	4.960	22.824	18.438	**24.788**	22.218	2.528	24.680	18.908	**26.245**
103 m	**29.689**	14.968	24.965	22.316	29.046	29.849	9.452	28.401	23.339	**29.703**
105 m	30.180	13.664	25.516	27.017	**30.379**	30.725	5.899	29.272	27.346	**31.730**
109 m	**31.761**	5.243	25.719	29.033	31.809	32.257	4.475	29.803	29.251	**33.823**
116 m	31.898	10.628	26.047	22.841	**31.996**	32.367	5.557	30.299	24.636	**34.193**
119 m	**35.157**	15.162	26.125	25.838	33.074	**36.255**	9.129	30.713	27.729	35.835
123 m	**36.793**	15.137	25.793	23.208	31.980	**38.502**	15.787	30.071	24.822	33.399
201 m	**29.574**	15.777	24.683	23.735	28.416	**29.807**	14.927	27.598	24.651	29.222
205 m	**32.686**	16.504	25.545	21.191	31.241	**33.818**	12.673	28.644	22.152	31.522
213 m	33.980	4.389	26.164	28.346	**34.088**	35.291	3.866	30.976	29.473	**38.299**
219 m	**33.658**	11.107	26.164	24.846	33.025	34.738	8.263	30.863	26.377	**35.884**
220 m	**30.517**	15.790	24.619	19.065	28.221	**31.084**	10.433	26.333	20.435	28.445
221 m	**28.205**	15.661	24.464	23.168	27.997	28.494	13.373	27.183	24.479	**28.715**
223 m	**35.146**	11.410	26.106	25.471	33.622	36.068	4.071	30.863	27.058	**37.238**
231 m	27.866	11.733	25.770	21.382	**29.300**	28.072	6.256	29.180	22.867	**30.194**
AVG	**30.952**	12.370	25.238	23.355	30.274	31.689	9.091	28.736	24.505	**31.903**

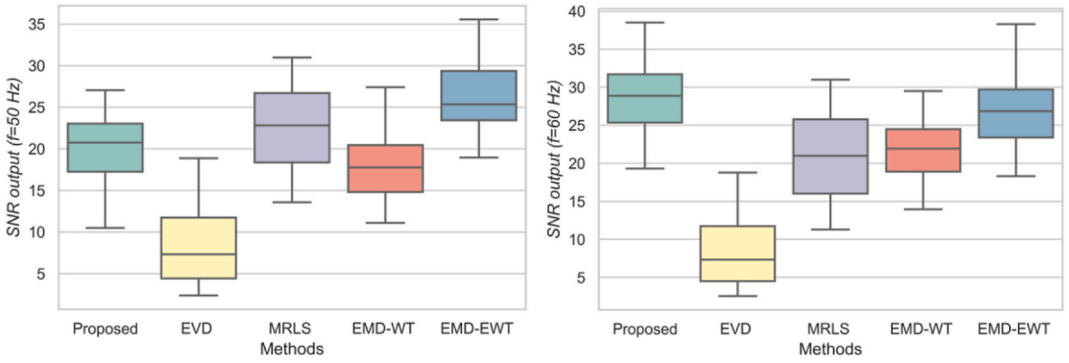


Fig. 11. PLI removal comparison, (a) SNR_{output} ($f = 50$ Hz), (b) SNR_{output} ($f = 60$ Hz).

Table 8
Comparative analysis of PSO-WT and GA-WT methods for PLI removal in ECG signals.

ECG record	SNR Input	SNR Output		MSE		RMSE		PRD (%)	
		PSO-WT	GA-WT	PSO-WT	GA-WT	PSO-WT	GA-WT	PSO-WT	GA-WT
100 m	5	**19.74**	15.78	**0.0014**	0.0035	**0.0373**	0.0589	**10.33**	16.46
	10	**22.48**	18.32	**0.0009**	0.0019	**0.0292**	0.0439	**8.08**	12.20
102 m	5	**18.11**	15.06	**0.0018**	0.0023	**0.0428**	0.0487	**15.89**	17.91
	10	**20.69**	17.52	**0.0015**	0.0017	**0.0382**	0.0395	**14.17**	14.89
103 m	5	**20.93**	14.39	**0.0017**	0.0045	**0.0412**	0.0673	**10.58**	19.41
	10	**23.95**	16.96	**0.0007**	0.0024	**0.0259**	0.0495	**6.65**	14.18
105 m	5	**24.13**	20.84	**0.0009**	0.0014	**0.0308**	0.0377	**8.04**	14.18
	10	**25.11**	21.00	**0.0011**	0.0012	**0.0328**	0.0348	**8.58**	8.94
109 m	5	**31.76**	24.7	**0.0008**	0.0010	**0.0287**	0.0348	**5.18**	5.82
	10	**32.25**	25.3	**0.0006**	0.0009	**0.0254**	0.0300	**4.59**	5.43

The experiments performed in this work show that noise suppression depends mainly on the appropriate wavelet family, decay level, and threshold techniques. PSO is a powerful tool for parameter selection and optimisation. Thus, the approach based on PSO and WT effectively reduces noise, outperforming other state-of-the-art techniques, according to the SNR, and making the clinical diagnosis more appropriate.

Future endeavours will centre around implementing our proposed approach on embedded systems with high computational resources, such as FPGA, to enhance its applicability in IoT-based applications. Furthermore, we will explore the potential of Particle Swarm Optimisation Variants, Hybrid Approaches, and Reinforcement Learning for Optimisation in maximising our proposed approach's performance on embedded systems. Additionally, we will rigorously assess the performance of this approach in real e-health applications, focusing on its effectiveness in filtering ECG signals in the presence of high-frequency noise—a challenge intricately linked to both hardware and environmental influences.

Data availability statement

Data associated with this study is available at https://physionet.org/about/database/.

CRediT authorship contribution statement

Abdallah Azzouz: Data curation, Formal analysis, Investigation, Methodology, Software, Writing – original draft, Writing – review & editing. **Billel Bengherbia:** Methodology, Supervision, Writing – original draft, Writing – review & editing. **Patrice Wira:** Funding acquisition, Investigation, Supervision, Writing – original draft, Validation. **Nail Alaoui:** Data curation, Formal analysis, Methodology, Software. **Abdelkerim Souahlia:** Formal analysis, Software, Writing – original draft. **Mohamed Maazouz:** Validation, Writing – review & editing. **Hamza Hentabeli:** Formal analysis, Investigation, Software, Visualization.

Declaration of competing interest

The authors declare the following financial interests/personal relationships which may be considered as potential competing interests: Abdallah AZZOUZ reports that the article publishing charges were provided by the Institute of Research in Computer Science,

Mathematics, Automation and Signal IRIMAS, Université de Haute Alsace, Mulhouse 68093, France.

References

[1] Y. Weiting, Z. Runjing, An improved self-adaptive filter based on LMS algorithm for filtering 50Hz interference in ECG signals, in: 2007 8th Int. Conf. Electron. Meas. Instruments, 2007, pp. 874–878, https://doi.org/10.1109/ICEMI.2007.4351057.

[2] S. Shadmand, B. Mashoufi, A new personalized ECG signal classification algorithm using Block-based Neural Network and Particle Swarm Optimization, Biomed. Signal Process Control 25 (2016) 12–23, https://doi.org/10.1016/j.bspc.2015.10.008.

[3] S. Farashi, A multiresolution time-dependent entropy method for QRS complex detection, Biomed. Signal Process Control 24 (2016) 63–71, https://doi.org/10.1016/j.bspc.2015.09.008.

[4] R. Tung, P. Zimetbaum, Use of the electrocardiogram in acute myocardial infarction, Card. Intensive Care (2010) 106–109, https://doi.org/10.1016/B978-1-4160-3773-6.10011-4.

[5] J.A. van Alsté, W. van Eck, O.E. Herrmann, ECG baseline wander reduction using linear phase filters, Comput. Biomed. Res. 19 (1986) 417–427, https://doi.org/10.1016/0010-4809(86)90037-6.

[6] I.P. Mitov, A method for reduction of power line interference in the ECG, Med. Eng. Phys. 26 (2004) 879–887, https://doi.org/10.1016/j.medengphy.2004.08.014.

[7] M.S. Chavan, R.A. Agarwala, M.D. Uplane, M.S. Gaikwad, Design of ECG instrumentation and implementation of digital filter for noise reduction, Recent Adv. Signal Process. Robot. Autom. (2004) 36–39.

[8] M.S. Chavan, R.A. Agarwala, M.D. Uplane, Suppression of baseline wander and power line interference in ECG using digital IIR filter, Int. J. Circuits, Syst. Signal Process. 2 (2008) 356–365.

[9] U. Biswas, M. Maniruzzaman, Removing power line interference from ECG signal using adaptive filter and notch filter, in: 2014 Int. Conf. Electr. Eng. Inf. Commun. Technol, 2014, pp. 1–4, https://doi.org/10.1109/ICEEICT.2014.6919072.

[10] A.-R. Al-Qawasmi, K. Daqrouq, ECG signal enhancement using wavelet transform, WSEAS Trans. Biol. Biomed. 7 (2010) 62–72.

[11] S.M.M. Martens, M. Mischi, S.G. Oei, J.W.M. Bergmans, An improved adaptive power line interference canceller for electrocardiography, IEEE Trans. Biomed. Eng. 53 (2006) 2220–2231, https://doi.org/10.1109/TBME.2006.883631.

[12] M.Z.U. Rahman, R.A. Shaik, D.V.R.K. Reddy, Efficient sign based normalized adaptive filtering techniques for cancelation of artifacts in ECG signals: application to wireless biotelemetry, Signal Process. 91 (2011) 225–239, https://doi.org/10.1016/j.sigpro.2010.07.002.

[13] M. Butt, N. Razzaq, I. Sadiq, M. Salman, T. Zaidi, Power Line Interference removal from ECG signal using SSRLS algorithm, in: 2013 IEEE 9th Int. Colloq. Signal Process. Its Appl, 2013, pp. 95–98, https://doi.org/10.1109/CSPA.2013.6530021.

[14] N. Kumaravel, N. Nithiyanandam, Genetic-algorithm cancellation of sinusoidal powerline interference in electrocardiograms, Med. Biol. Eng. Comput. 36 (1998) 191–196, https://doi.org/10.1007/BF02510742.

[15] J. Mateo, C. Sanchez, A. Tortes, R. Cervigon, J.J. Rieta, Neural network based canceller for powerline interference in ECG signals, in: 2008 Comput. Cardiol, 2008, pp. 1073–1076, https://doi.org/10.1109/CIC.2008.4749231.

[16] N.E. Huang, Z. Shen, S.R. Long, M.C. Wu, H.H. Shih, Q. Zheng, N.-C. Yen, C.C. Tung, H.H. Liu, The empirical mode decomposition and the Hilbert spectrum for nonlinear and non-stationary time series analysis, Proc. R. Soc. London. Ser. A Math. Phys. Eng. Sci. 454 (1998) 903–995, https://doi.org/10.1098/rspa.1998.0193.

[17] A.J. Nimunkar, W.J. Tompkins, EMD-based 60-Hz noise filtering of the ECG, in: 2007 29th Annu. Int. Conf. IEEE Eng. Med. Biol. Soc, 2007, pp. 1904–1907, https://doi.org/10.1109/IEMBS.2007.4352688.

[18] Z. Zhidong, M. Chan, A novel cancellation method of powerline interference in ECG signal based on EMD and adaptive filter, in: 2008 11th IEEE Int. Conf. Commun. Technol, 2008, pp. 517–520, https://doi.org/10.1109/ICCT.2008.4716100.

[19] M. Suchetha, N. Kumaravel, Empirical mode decomposition based filtering techniques for power line interference reduction in electrocardiogram using various adaptive structures and subtraction methods, Biomed. Signal Process Control 8 (2013) 575–585, https://doi.org/10.1016/j.bspc.2013.05.001.

[20] A.K. Ziarani, A. Konrad, A nonlinear adaptive method of elimination of power line interference in ECG signals, IEEE Trans. Biomed. Eng. 49 (2002) 540–547, https://doi.org/10.1109/TBME.2002.1001968.

[21] M.A. Kabir, C. Shahnaz, Denoising of ECG signals based on noise reduction algorithms in EMD and wavelet domains, Biomed. Signal Process Control 7 (2012) 481–489, https://doi.org/10.1016/j.bspc.2011.11.003.

[22] Y. Kopsinis, S. McLaughlin, Development of EMD-based denoising methods inspired by wavelet thresholding, IEEE Trans. Signal Process. 57 (2009) 1351–1362, https://doi.org/10.1109/TSP.2009.2013885.

[23] K.-M. Chang, Arrhythmia ECG noise reduction by ensemble empirical mode decomposition, Sensors 10 (2010) 6063–6080, https://doi.org/10.3390/s100606063.

[24] M.R. Keshtkaran, Z. Yang, A fast, robust algorithm for power line interference cancellation in neural recording, J. Neural. Eng. 11 (2014) 1–18, https://doi.org/10.1088/1741-2560/11/2/026017.

[25] J. Piskorowski, Digital notch filter with time-varying quality factor for the reduction of powerline interference, in: Proc. 2010 IEEE Int. Symp. Circuits Syst, 2010, https://doi.org/10.1109/ISCAS.2010.5537032, 2706–2709.

[26] S. Boda, M. Mahadevappa, P.K. Dutta, A hybrid method for removal of power line interference and baseline wander in ECG signals using EMD and EWT, Biomed. Signal Process Control 67 (2021) 102466, https://doi.org/10.1016/j.bspc.2021.102466.

[27] S. Agrawal, A. Gupta, Fractal and EMD based removal of baseline wander and powerline interference from ECG signals, Comput. Biol. Med. 43 (2013) 1889–1899, https://doi.org/10.1016/j.compbiomed.2013.07.030.

[28] R.R. Sharma, R.B. Pachori, Baseline wander and power line interference removal from ECG signals using eigenvalue decomposition, Biomed. Signal Process Control 45 (2018) 33–49, https://doi.org/10.1016/j.compbiomed.2013.07.030.

[29] S. Kumar, D. Panigrahy, P.K. Sahu, Denoising of Electrocardiogram (ECG) signal by using empirical mode decomposition (EMD) with non-local mean (NLM) technique, Biocybern. Biomed. Eng. 38 (2018) 297–312, https://doi.org/10.1016/j.bbe.2018.01.005.

[30] S.L. Joshi, R.A. Vatti, R. V Tornekar, A survey on ECG signal denoising techniques, in: 2013 Int. Conf. Commun. Syst. Netw. Technol, 2013, pp. 60–64, https://doi.org/10.1109/CSNT.2013.22.

[31] B.H. Tracey, E.L. Miller, Nonlocal means denoising of ECG signals, IEEE Trans. Biomed. Eng. 59 (2012) 2383–2386, https://doi.org/10.1109/TBME.2012.2208964.

[32] S. Samadi, M.B. Shamsollahi, ECG noise reduction using empirical mode decomposition based on combination of instantaneous half period and soft-thresholding, Middle East Conf. Biomed. Eng. MECBME. (2014) 244–248, https://doi.org/10.1109/MECBME.2014.6783250.

[33] A. Chacko, S. Ari, Denoising of ECG signals using Empirical Mode Decomposition based technique, in: IEEE-international Conf. Adv. Eng. Sci. Manag. ICAESM-2012 vol. 2, 2012, pp. 6–9.

[34] M. Rakshit, S. Das, An efficient ECG denoising methodology using empirical mode decomposition and adaptive switching mean filter, Biomed. Signal Process Control 40 (2018) 140–148, https://doi.org/10.1016/j.bspc.2017.09.020.

[35] R.N. Vargas, A.C.P. Veiga, Electrocardiogram signal denoising by clustering and soft thresholding, IET Signal Process. 12 (2018) 1165–1171, https://doi.org/10.1049/iet-spr.2018.5162.

[36] G. Han, Z. Xu, Electrocardiogram signal denoising based on a new improved wavelet thresholding, Rev. Sci. Instrum. 87 (2016) 1–7, https://doi.org/10.1063/1.4960411.

[37] L. Condat, A direct algorithm for 1-D total variation denoising, IEEE Signal Process. Lett. 20 (2013) 1054–1057, https://doi.org/10.1109/LSP.2013.2278339.

[38] R.N. Vargas, A.C.P. Veiga, Electrocardiogram signal denoising by a new noise variation estimate, Res. Biomed. Eng. 36 (2020) 13–20, https://doi.org/10.1007/s42600-019-00033-y.
[39] E.S.A. El-Dahshan, Genetic algorithm and wavelet hybrid scheme for ECG signal denoising, Telecommun. Syst. 46 (2011) 209–215, https://doi.org/10.1007/s11235-010-9286-2.
[40] Z.A.A. Alyasseri, A.T. Khader, M.A. Al-Betar, A.K. Abasi, S.N. Makhadmeh, EEG signals denoising using optimal wavelet transform hybridized with efficient metaheuristic methods, IEEE Access 8 (2020) 10584–10605, https://doi.org/10.1109/ACCESS.2019.2962658.
[41] S. Masoodian, A. Bazrafshan, H. Rajabi Mashhadi, Biomedical signal denoising by adaptive wavelet design using genetic algorithms, in: ICEE 2012 - 20th Iran. Conf. Electr. Eng, 2012, pp. 1590–1593, https://doi.org/10.1109/IranianCEE.2012.6292614.
[42] Y. Xingwei, L. Dawei, Y. Afeng, Z. Jun, C. Du, A novel method of wavelet threshold shrinkage based on genetic algorithm and sample entropy, in: Proc. 2013 3rd Int. Conf. Intell. Syst. Des. Eng. Appl. ISDEA, 2013, pp. 144–149, https://doi.org/10.1109/ISDEA.2012.41, 2013.
[43] H. Nagendra, S. Mukherjee, V. Kumar, Application of wavelet techniques in ECG signal processing: an overview, Int. J. Eng. Sci. Technol. 3 (2011) 7432–7443.
[44] M. Vozda, F. Jurek, M. Cerny, Individualization of a vectorcardiographic model by a particle swarm optimization, Biomed. Signal Process Control 22 (2015) 65–73, https://doi.org/10.1016/j.bspc.2015.06.010.
[45] H. Mirvaziri, Z.S. Mobarakeh, Improvement of EEG-based motor imagery classification using ring topology-based particle swarm optimization, Biomed. Signal Process Control 32 (2017) 69–75, https://doi.org/10.1016/j.bspc.2016.10.015.
[46] H.D. Hesar, A.D. Hesar, ECG enhancement using a modified Bayesian framework and particle swarm optimization, Biomed. Signal Process Control 80 (2023) 1–12, https://doi.org/10.1016/j.bspc.2022.104280.
[47] W. Zhang, Z. Lin, X. Liu, Short-term offshore wind power forecasting - a hybrid model based on discrete wavelet transform (DWT), seasonal autoregressive integrated moving average (sarima), and deep-learning-based long short-term memory (lstm), Renew. Energy 185 (2022) 611–628, https://doi.org/10.1016/j.renene.2021.12.100.
[48] M. Rouis, S. Sbaa, N.E. Benhassine, The effectiveness of the choice of criteria on the stationary and non-stationary noise removal in the phonocardiogram (PCG) signal using discrete wavelet transform, Biomed. Tech. 65 (2020) 353–366, https://doi.org/10.1515/bmt-2019-0197.
[49] Z.A.A. Alyasseri, A.T. Khader, M.A. Al-Betar, Electroencephalogram signals denoising using various mother wavelet functions: a comparative analysis, in: ACM Int. Conf. Proceeding Ser., Association for Computing Machinery, 2017, pp. 100–105, https://doi.org/10.1145/3132300.3132313.
[50] C. Sawant, H.T. Patii, Wavelet based ECG signal de-noising, in: 1st Int. Conf. Networks Soft Comput, ICNSC 2014 - Proc., 2014, pp. 20–24, https://doi.org/10.1109/CNSC.2014.6906684.
[51] D.L. Donoho, J.M. Johnstone, Ideal spatial adaptation by wavelet shrinkage, Biometrika 81 (1994) 425–455, https://doi.org/10.1093/biomet/81.3.425.
[52] B.N. Singh, A.K. Tiwari, Optimal selection of wavelet basis function applied to ECG signal denoising, Digit. Signal Process. 16 (2006) 275–287, https://doi.org/10.1016/j.dsp.2005.12.003.
[53] M. Rakibul Mowla, S.C. Ng, M.S.A. Zilany, R. Paramesran, Artifacts-matched blind source separation and wavelet transform for multichannel EEG denoising, Biomed. Signal Process Control 22 (2015) 111–118, https://doi.org/10.1016/j.bspc.2015.06.009.
[54] S.M. Isa, A. Noviyanto, A.M. Arymurthy, Optimal selection of wavelet thresholding algorithm for ECG signal denoising, in: ICACSIS 2011 - 2011 Int. Conf. Adv. Comput. Sci. Inf. Syst. Proc, 2011, pp. 365–370.
[55] D.L. Donoho, De-noising by soft-thresholding, IEEE Trans. Inf. Theor. 41 (1995) 613–627, https://doi.org/10.1109/18.382009.
[56] R. Poli, J. Kennedy, T. Blackwell, Quantification & Assessment of the chemical form of residual gadolinium in the brain, Swarm. Intell. 1 (2007) 33–57, https://doi.org/10.1007/s11721-007-0002-0.
[57] D. Wang, D. Tan, L. Liu, Particle swarm optimization algorithm: an overview, Soft Comput. 22 (2018) 387–408, https://doi.org/10.1007/s00500-016-2474-6.
[58] MIT-BIH database. http://www.physionet.org/physiobank/database/mitdb, 2023. (Accessed 15 September 2023).
[59] V. Prasad, P. Siddaiah, B.P. Rao, A new wavelet based method for denoising of biological signals, Int. J. Comput. Sci. Netw. Secur. 8 (2008) 238–244.
[60] S. Chatterjee, R.S. Thakur, R.N. Yadav, L. Gupta, D.K. Raghuvanshi, Review of noise removal techniques in ECG signals, IET Signal Process. 14 (2020) 569–590, https://doi.org/10.1049/iet-spr.2020.0104.
[61] A. Abdallah, B. Billel, A. Nail, S. Abdelkerim, ECG signal denoising based on wavelet transform and genetic algorithm, in: 2023 Int. Conf. Adv. Electron. Control Commun. Syst, 2023, pp. 1–6, https://doi.org/10.1109/ICAECCS56710.2023.10105043.